THE JOURNAL OF BIOLOGICAL CHEMISTRY
Vol. 277, No. 1, Issue of January 4, pp. 272–278, 2002
Printed in U.S.A.


# The Linker Domain of the Ha-Ras Hypervariable Region Regulates Interactions with Exchange Factors, Raf-1 and Phosphoinositide 3-Kinase*

Received for publication, August 31, 2001, and in revised form, October 3, 2001
Published, JBC Papers in Press, October 31, 2001, DOI 10.1074/jbc.M108423200

**Montserrat Jaumot‡, Jun Yan‡, Jodi Clyde-Smith, Judith Sluimer, and John F. Hancock§**

*From the Laboratory of Experimental Oncology, Department of Pathology, University of Queensland Medical School, Herston Road, Queensland 4006, Australia*

**Ha-Ras and Ki-Ras have different distributions across plasma membrane microdomains. The Ras C-terminal anchors are primarily responsible for membrane microlocalization, but recent work has shown that the interaction of Ha-Ras with lipid rafts is modulated by GTP loading via a mechanism that requires the hypervariable region (HVR). We have now identified two regions in the HVR linker domain that regulate Ha-Ras raft association. Release of activated Ha-Ras from lipid rafts is blocked by deleting amino acids 173–179 or 166–172. Alanine replacement of amino acids 173–179 but not 166–172 restores wild type micro-localization, indicating that specific N-terminal sequences of the linker domain operate in concert with a more C-terminal spacer domain to regulate Ha-Ras raft association. Mutations in the linker domain that confine activated Ha-RasG12V to lipid rafts abrogate Raf-1, phosphoinositide 3-kinase, and Akt activation and inhibit PC12 cell differentiation. *N*-Myristoylation also prevents the release of activated Ha-Ras from lipid rafts and inhibits Raf-1 activation. These results demonstrate that the correct modulation of Ha-Ras lateral segregation is critical for downstream signaling. Mutations in the linker domain also suppress the dominant negative phenotype of Ha-RasS17N, indicating that HVR sequences are essential for efficient interaction of Ha-Ras with exchange factors in intact cells.**

The guanine nucleotide-binding protein Ras acts as a molecular switch connecting extracellular signals with a complex network of intracellular signal transduction pathways that mediate a variety of cellular responses including proliferation and differentiation (1, 2). The three mammalian *ras* genes encode for four proteins of 188 and 189 amino acids (Ha-Ras, N-Ras, Ki-RasA, Ki-RasB) that are identical over the N-terminal 85 amino acids and 90% homologous over the next 80 residues. These N-terminal 165 residues are sufficient for binding guanine nucleotides and interacting with effector and exchange factor proteins *in vitro*. The divergence between the Ras isoforms is largely confined to the final 23 and 24 C-terminal amino acids, the so-called hypervariable region (HVR)[1] in which less than 10–15% of residues are identical between any pair of Ras proteins.

The localization of Ras to the inner surface of the plasma membrane is essential for its biological activity (3). The two signals responsible for the correct plasma membrane localization of Ras are contained in the Ras HVR. The first signal sequence, common to all Ras proteins, is the C-terminal C*AAX* box (in which *A* = aliphatic amino acid and *X* = serine or methionine) that is sequentially farnesylated, -*AAX* proteolyzed, and carboxyl-methylated (3–6). This series of posttranslational modifications is completed on the cytoplasmic surface of the endoplasmic reticulum. The second signal comprises palmitoylation of two upstream cysteines ($Cys^{181}$ and $Cys^{184}$) in Ha-Ras, one cysteine ($Cys^{181}$) in N-Ras, and a polybasic sequence of multiple lysines ($Lys^{175–180}$) in Ki-Ras[2] (7, 8). These targeting signals direct the trafficking of Ras to the cell surface via alternative routes. After palmitoylation, probably also in the endoplasmic reticulum, Ha- and N-Ras traffic through the classical exocytic pathway via the Golgi to the plasma membrane (9, 10). Ki-Ras in contrast bypasses the Golgi and reaches the plasma membrane by an unknown mechanism that may involve transport or simple diffusion (9–13). For convenience we refer to the sequences of the Ras HVR that are involved in trafficking and plasma membrane attachment as the membrane-targeting domain and the remainder of the Ras HVR as the linker domain.

A number of studies have shown that the membrane-targeting domains localize Ha-Ras and Ki-Ras to different microdomains of the plasma membrane. A dominant negative mutant of caveolin, $Cav^{DGV}$, which blocks delivery of cholesterol to the plasma membrane (14), completely blocks Ha-Ras-dependent Raf activation but does not affect Ki-Ras signaling (15). The inhibition is reversed by repleting plasma membranes with cholesterol. In addition, chemically depleting plasma membrane cholesterol with cyclodextrin selectively inhibits Ha-Ras but not Ki-Ras function (15). Taken together, these data suggest that Ha-Ras but not Ki-Ras function is dependent on the integrity of lipid rafts in the plasma membrane. More recently we used electron and fluorescent microscopy coupled with biochemical fractionation to examine the plasma membrane microdomain distributions of Ha- and Ki-Ras (16). The results were unexpected but clear. The C-terminal minimal membrane-targeting sequences of Ha-Ras localize GFP to caveolae and lipid rafts, whereas the equivalent targeting signals for

* This work was supported by grants from the National Health and Medical Research Council of Australia. The costs of publication of this article were defrayed in part by the payment of page charges. This article must therefore be hereby marked "*advertisement*" in accordance with 18 U.S.C. Section 1734 solely to indicate this fact.

‡ These authors contributed equally to this work.

§ Supported by the Royal Children's Hospital Foundation, Queensland. To whom correspondence should be addressed: Tel.: 61-7-3365-5288; Fax: 61-7-3365-5511; E-mail: j.hancock@mailbox.uq.edu.au.

[1] The abbreviations used are: HVR, hypervariable region; PI3K, phosphoinositide 3-kinase; GFP, green fluorescent protein; GEF, guanine nucleotide exchange factor; BHK, baby hamster kidney; MAP, mitogen-activated protein; MAPK, MAP kinase; ERK, extracellular signal-regulated kinase; MEK, MAPK/ERK kinase; RBD, Ras-binding domain.

[2] The major expressed Ki-Ras protein is Ki-RasB, referred to as Ki-Ras hereafter.

Ki-Ras do not. Wild type GDP-bound Ha-Ras is distributed equally between lipid raft and non-raft membrane, but constitutively activated GTP-bound Ha-Ras is almost completely excluded from lipid rafts and caveolae. In contrast, GDP- and GTP-loaded Ki-Ras are both absent from caveolae and co-fractionate with markers of disordered plasma membrane. The data suggest that Ha-Ras is in a GTP-regulated equilibrium between lipid rafts and non-raft plasma membrane (16, 17). Interestingly, the Ha-Ras linker domain is necessary for the GTP-dependent release of Ha-Ras from lipid rafts and for biological activity (16). Other studies have also shown that manipulation of the C-terminal membrane anchor of Ha-Ras decreases Ras biological activity in NIH3T3 and PC12 cells by changing effector pathway utilization (18, 19). Together these observations demonstrate that the integrity of the HVR is essential for normal Ha-Ras signaling.

The aim of the present study was to investigate in more detail the role of the HVR linker domain in Ha-Ras function. In particular we wanted to establish what structural features and/or specific sequences in the linker domain contribute to the modulation of Ha-Ras raft association and to examine whether raft association alone determines the efficiency with which Ha-Ras interacts with specific effectors and activators. These are important questions because differential distribution of Ras isoforms, exchange factors, effectors, and effector co-activators across plasma membrane microdomains is the simplest mechanism that can account for the increasing number of biological and *in vivo* biochemical differences that are being identified between Ha-, Ki-, and N-Ras.

## EXPERIMENTAL PROCEDURES

*Plasmids*—Ha-RasG12V cDNA sequences encoding $His^{166}$ though $Asn^{172}$ or $Pro^{173}$ though $Pro^{179}$ were deleted or replaced with polyalanine using oligonucleotide-directed mutagenesis to generate HΔ1-G12V, HΔ1ala-G12V, HΔ2-G12V, and HΔ2ala-G12V, respectively. Mutated cDNAs were fully sequenced and cloned into the expression vector pEXV3, $Gly^{12}$, and $Asn^{17}$ versions of the HVR mutants were constructed by recombination with pEXV-Ha-Ras and pEXV-Ha-RasS17N, respectively. EXV-HΔhvr-G12V and EXV-Mys-Ha-Ras have been described previously (16, 20).

*Cell Culture and Transfection*—BHK cells were cultured at 37 °C in Dulbecco's modified Eagle's medium (DMEM) supplemented with 10% bovine calf serum. Cells were plated onto 10-cm plates at 60% confluence and transfected with 5–10 μg of expression plasmid using LipofectAMINE (Invitrogen) according to the manufacturer's instructions. After 5 h of incubation with the transfection mix, medium containing 20% calf serum was added for an overnight incubation. Next day, the cells were incubated for 6 h in serum-free medium and then processed. PC12 cells were cultured in DMEM supplemented with 5% horse serum, 10% calf serum, and 2 mM L-glutamine and were transfected using LipofectAMINE. 16 h after lipofection, the cells were returned to standard PC12 maintenance medium and were incubated a further 48 h prior to processing for confocal microscopy. COS cells were cultured in DMEM supplemented with 10% bovine calf serum at 37 °C. The cells were electroporated with expression plasmids, and after 48 h, they were serum-starved for 16 h before being harvested for the GTP-loading assays.

*Cell Fractionation*—Transfected BHK and COS cells were washed with cold phosphate-buffered saline, scraped on ice into 0.3 ml of Buffer A (10 mM Tris-Cl, pH 7.5, 5 mM $MgCl_2$, 1 mM EGTA, 1 mM dithiothreitol, 100 μM $NaVO_4$, 25 mM NaF, 10 μg/ml leupeptin, and 10 μg/ml aprotinin), and homogenized through a 23-gauge needle. Post-nuclear supernatants obtained by low speed centrifugation were spun at 100,000 × *g* at 4 °C for 30 min, and the soluble fraction (S100), which contains cytosolic proteins, was collected. The sedimented fraction (P100), which contains cellular membranes, was rinsed and resuspended in 100 μl of Buffer A.

*Western Blotting*—Protein content was measured by the Bradford reaction. 20 μg each of S100 and P100 fraction was separated in 10 and 12% SDS-polyacrylamide gels and transferred to polyvinylidene difluoride membranes. Western blotting was performed using the following antibodies: Ras (Y13–259), Phospho-MEK1/2 ($Ser^{217/221}$) (No. 9121 Cell Signaling), Phospho-p44/42 MAP kinase ($Thr^{202}$/$Tyr^{204}$) (No. 9106S, Cell Signaling), or Phospho-Akt ($Ser^{473}$) (No. 9271S, Cell Signaling). Western blots were developed using horseradish peroxidase-conjugated secondary antibodies and ECL (SuperSignal; Pierce) and quantified by phosphorimaging with a CH-screen (Bio-Rad).

*Confocal Microscopy*—Transfected PC12 or BHK cells were washed with phosphate-buffered saline and fixed with 4% paraformaldehyde for 30 min at room temperature. Indirect anti-Ras immunofluorescence using Y13–238 and FITC-coupled anti-rat secondary antisera was performed as described previously (10). Coverslips were mounted in mowiol for confocal microscopy.

*Raf-1 Kinase Assays*—Raf activity was measured in a coupled MEK/ERK assay with myelin basic protein phosphorylation as readout exactly as described (21).

*Sucrose Gradients*—Cell membranes were resolved in bottom-loaded continuous sucrose gradients exactly as described (16, 22).

*Phosphoinositide 3-Kinase (PI3K) Assays*—Transfected BHK cells were serum-starved for 6 h, harvested, and fractionated into S100 and P100 fractions. 400 μg of each P100 fraction was collected by centrifuging at 100,000 × *g* at 4 °C for 30 min. The membrane pellets were resuspended by sonication in 100 μl of lysis buffer (50 mM HEPES, pH 7.5, 150 mM NaCl, 10% glycerol, 1% Triton X-100, 1.5 mM $MgCl_2$, 1 mM EGTA, 10 mM $Na_4P_2O_7$, 100 mM sodium fluoride, 10 μg/ml aprotinin, 10 μg/ml leupeptin, 1 mM phenylmethylsulfonyl fluoride, and 1 mM $NaVO_4$), and after a 15-min incubation on ice, they were recentrifuged at 100,000 × *g* at 4 °C for 20 min. The supernatants were discarded, and the new pellets were resuspended by sonication in 25 μl of 2× kinase buffer (40 mM Tris-Cl, pH 7.6, 150 mM NaCl, and 20 mM $MgCl_2$). 25 μl of kinase mix (phosphatidylinositol, 200 μg/ml sonicated in 20 mM HEPES, pH 7.5, 20 μM ATP, 200 μM adenosine, and 10 μCi of [γ-$^{32}$P]ATP (6,000 Ci/mmol)) was added, and kinase reactions were carried out for 20 min at 25 °C in a vortexing heating block. Reactions were stopped with 100 μl of 1 N HCl, and phospholipids were extracted once with 200 μl of $CHCl_3$:MeOH (1:1) and once with 160 μl of 1 N HCl:MeOH (1:1). Phosphorylated lipid products were resolved on oxalate-impregnated Silica60 plates (Merck) using $CHCl_3$:MeOH:4 M $NH_4OH$ (9:7:2) as solvent and visualized and quantified by phosphorimaging with a BI screen (Bio-Rad).

*Triton Solubility Assay*—Cells were transfected, harvested, and fractionated as described above. Aliquots of P100 fraction were added to a dilution range of Triton X-100 in Buffer Q (25 mM Tris-Cl, pH 7.5, 5 mM $MgCl_2$, and 25 mM KCl) to obtain a final concentration of 0, 0.05, 0.25, and 0.5% Triton X-100. The samples were then sonicated for 15 s, incubated on ice for 15 min, sonicated again for 10 s, and centrifuged at 100,000 × *g* for 30 min. The supernatants were discarded, and the pellets were dissolved in sample buffer, resolved on 15% SDS-polyacrylamide gels, and immunoblotted for Ras.

*GTP-loading Assays*—S100 and P100 fractions were prepared from COS cells transfected as described above. The P100 fractions were resuspended in 400 μl of lysis buffer (20 mM Tris-Cl, pH 7.5, 150 mM NaCl, 0.5% Triton X-100, 0.5% sodium deoxycholate, 10 μg/ml aprotinin, and 1 mM phenylmethylsulfonyl fluoride), sonicated, and then spun at 14,000 rpm at 4 °C for 5 min, and soluble supernatants were moved to new tubes. Protein content was measured by the Bradford reaction, and 120 μg of the sample was incubated with 1 ml of binding buffer (50 mM Tris-Cl, pH 7.5, 10 mM $MgCl_2$, 0.5 mg/ml bovine serum albumin, 0.5 mM dithiothreitol, and 100 mM NaCl) and 20 μl of GST·RBD K85A fusion protein (50% suspension = 20 μg) for 90 min at 4 °C. For details, see Ref. 23. After washing three times with binding buffer, the final pellet was resuspended in 20 μl of 2× sample buffer, boiled, and loaded in 15% gels for Western blotting analysis using anti-Ras antibodies. 10 μg of the solubilized P100 fraction was also immunoblotted to normalize for total Ras content. After quantifying the immunoblots in a phosphorimaging device, GTP loading was estimated by calculating (RBD-bound Ras)/(total Ras present in 10 μg of solubilized P100 fraction). The phosphorimaging device units are arbitrary, but our previous comparisons of estimating GTP loading using the RBD pull-down assay with GTP loading measured by $^{32}$P labeling, Ras immunoprecipitation, and TLC have shown that 10 arbitrary units = ~2% GTP-bound Ras.

*Toxicity Assays*—BHK cells were transfected with 10 μg of S17N-substituted plasmid plus 0.8 μg of pC1 (which carries a G418-selectable marker). After 5 h, medium containing 20% calf serum was added for 24 h, and then the transfected cells were split between eight 10-cm plates into medium containing 10% calf serum and 500 μg/ml G418. Cells were maintained for 16 days and then fixed with cold methanol and stained with 10% Geimsa's stain, and the colonies were counted.

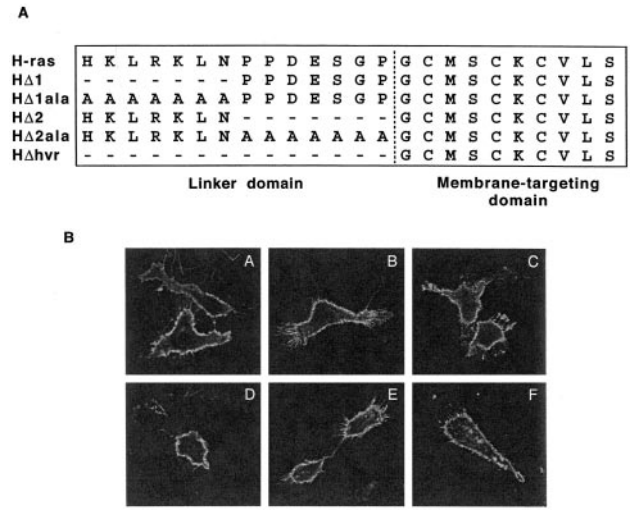


FIG. 1. **The Ha-Ras HVR linker domain mutants localize at the plasma membrane.** *A*, Ha-RasG12V HVR linker domain mutants HΔ1-G12V and HΔ2-G12V were constructed by deleting Ha-RasG12V cDNA sequences encoding $His^{166}$ though $Asn^{172}$ or $Pro^{173}$ though $Pro^{179}$, respectively. Mutants HΔ1ala-G12V and HΔ2ala-G12V were generated by replacing the above sequences with polyalanine. The HΔhvrG12V mutant consists of a deletion of the entire linker domain of Ha-Ras (166–179). The membrane-targeting sequences remain intact in these proteins. *B*, confocal images of BHK cells transiently expressing Ha-RasG12V (*A*), HΔ2-G12V (*B*), HΔ2ala-G12V (*C*), HΔ1-G12V (*D*), HΔ1ala-G12V (*E*), and HΔhvrG12V (*F*). All Ha-Ras HVR linker domain mutants localize to the plasma membrane.

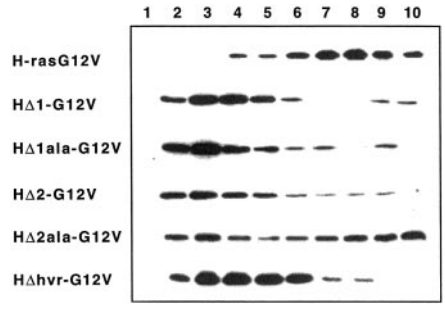


FIG. 2. **Distribution of Ha-Ras HVR linker domain mutants on sucrose gradients.** Carbonate lysates of cells transiently expressing Ha-RasG12V or the HVR linker domain mutants were sonicated and fractionated over sucrose gradients. 10 fractions, *numbered* from the *top* to the *bottom* of the gradient, were collected. These fractions were recentrifuged to isolate cell membranes, and the membrane pellets were immunoblotted for Ras. Note that all HVR linker domain mutants, except HΔ2ala-G12V, exclusively localize to the lipid raft-containing fractions (*top 5* fractions of the gradient). Full-length Ha-RasG12V and HΔ2ala-G12V are found predominantly in the non-raft enriched fractions (*bottom 5* fractions of the gradient).

## RESULTS

*Identification of Two Regions within the Ha-Ras HVR Linker Domain That Regulate Raft Association*—Our previous results showed that deletion of the entire linker domain of Ha-Ras (166–179) totally confines activated HΔhvrG12V to lipid rafts and partially abrogates the ability of HΔhvrG12V to activate Raf-1 (16). To further characterize the HVR linker domain, we constructed four additional mutants of this region. We deleted amino acids 166–172 or 173–179 from activated Ha-RasG12V, *i.e.* the N-terminal or C-terminal amino acids of the linker domain, to create the mutants HΔ1 and HΔ2, respectively (Fig. 1). In addition, we generated two alanine replacement mutants by substituting the amino acids 166–172 or 173–179 with an equivalent number of alanine residues to generate HΔ1ala and HΔ2ala (Fig. 1). The membrane-targeting domain of the HVR is left intact in all these constructs, and Fig. 1*B* shows that as expected, all of the Ha-Ras HVR-mutated proteins localized normally to the plasma membrane when expressed in BHK cells.

We next examined the distribution of the Ha-Ras linker domain mutants between raft and non-raft membranes. Detergent-free lysates prepared from transiently transfected BHK cells were fractionated over sucrose gradients. 10 fractions were collected from the top to the bottom of each gradient, and the membranes contained in each fraction isolated by centrifugation. Membrane pellets were then analyzed by immunoblotting using anti-Ras antibodies. We have previously extensively characterized this gradient protocol and shown that lipid raft-enriched membranes are readily resolved from non-raft membranes (16, 22). Specifically, lipid raft markers are found in the top 5 fractions of the gradients, which contain light membranes, and non-raft markers are confined to the denser bottom 5 fractions (16, 22).

In accordance with our previous results, more than 80% of activated Ha-RasG12V was present in the high density fractions (6–9) and was totally excluded from the top fractions of the gradient (Fig. 2). In contrast, the truncated proteins HΔ1-G12V and HΔ2-G12V and the alanine-substituted protein HΔ1ala-G12V fractionated almost exclusively to the lipid raft-enriched fractions (2–5) as seen previously for HΔhvrG12V (see Fig. 2 and Ref. 16). Interestingly, however, the distribution of the alanine-substituted protein HΔ2ala-G12V more closely resembled that of full-length Ha-RasG12V with a small peak in lipid raft fractions 2 and 3 and a more major peak in fractions 7–10. One interpretation of these results is that the whole Ha-Ras linker domain is required for correct lateral segregation, but although the specific amino acid sequence of 166–172 is critical, residues 173–179 may just operate as an essential spacer element, the specific sequence of which is not important.

*Correlation of Raft Micro-localization with Biochemical Activity*—To characterize the potential biological implications of defective membrane micro-localization, we examined the ability of the HVR mutants to activate downstream effectors. Membrane (P100) fractions from BHK cells transiently transfected with full-length Ha-RasG12V or the HVR linker domain mutants were normalized for Ras content and assayed for Raf-1 activity using a coupled MEK-ERK assay. Fig. 3, *A* and *B*, shows that the ability of HΔ1-G12V and HΔ2-G12V to activate Raf-1 was severely compromised compared with that of full-length Ha-RasG12V. The abrogation of activity was similar to that seen with HΔhvrG12V. The ability of HΔ1ala-G12V to activate Raf-1 was also compromised but not to the same extent as HΔ1-G12V, HΔ2-G12V, or HΔhvrG12V (Fig. 3, *A* and *B*). In contrast, the alanine replacement mutant HΔ2ala-G12V activated Raf-1 as efficiently as full-length Ha-RasG12V (Fig. 3, *A* and *B*). We next examined the levels of activated MEK and ERK in the S100 fractions of the same lysates by immunoblotting with phospho-specific antisera. Fig. 3*A* shows that MEK phosphorylation was significantly compromised only in cells expressing HΔhvrG12V. Moreover, levels of phosphorylated ERK were essentially equivalent in all of the mutant-expressing cells. Thus recruitment of Raf to lipid rafts by mislocalized Ha-Ras compromises activation but also apparently interferes with the communication between Raf, MEK, and MAPK, perhaps by preventing appropriate negative feedback within the kinase cascade.

Membrane fractions were then assayed for endogenous PI3K activity in an *in vitro* lipid kinase assay using phosphatidylinositol as substrate. Expression of HΔhvrG12V, HΔ1-G12V, and HΔ2-G12V failed to activate PI3K, whereas expression of HΔ2ala-G12V or full-length Ha-RasG12V generated substantial membrane-associated PI3K activity (Fig. 3, *C* and *D*). Ex-

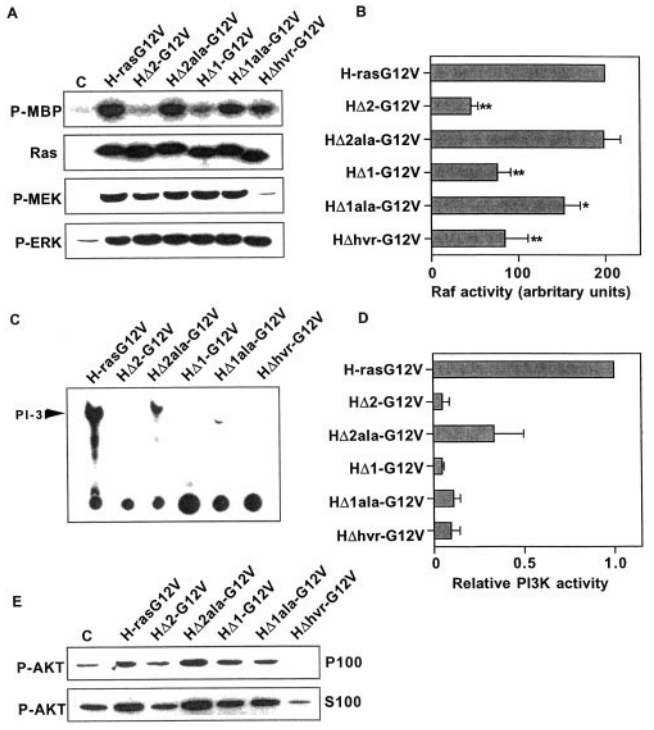


FIG. 3. **Biochemical activities of Ha-Ras HVR linker mutants.** BHK cells expressing Ha-RasG12V or HVR linker domain mutants or transfected with empty EXV vector as control were fractionated. P100 fractions were immunoblotted for Ras and assayed for Raf activity using a coupled MEK-ERK assay (*A*). An autoradiograph of a representative Raf assay is shown as phosphorylated myelin basic protein (*P-MBP*). S100 fractions from the same cells were then immunoblotted for activated MEK (*P-MEK*) and Erk (*P-Erk*) with phospho-specific antisera. The graph shows mean Raf activity (+ S.E., $n = 3$) in arbitrary phosphorimaging device units (*B*). Differences between each mean and the Ha-RasG12V control were examined in *t* tests; significant differences are indicated by * ($p < 0.05$) or ** ($p < 0.01$). PI3K activity in the cell membranes was measured in an *in vitro* lipid kinase assay using phosphatidylinositol as substrate (*C*). The phosphorylated products were resolved by TLC, and the position of PI-3P is marked with an *arrow*. PI3K assays were quantified by phosphorimaging the TLC plates. (*D*) The graph shows mean relative PI3K (+ S.E.) calculated from 3 or 4 independent experiments. Levels of activated Akt in P100 and S100 fractions of the same cell lysates were analyzed by immunoblotting with a phospho-specific antisera (*E*).

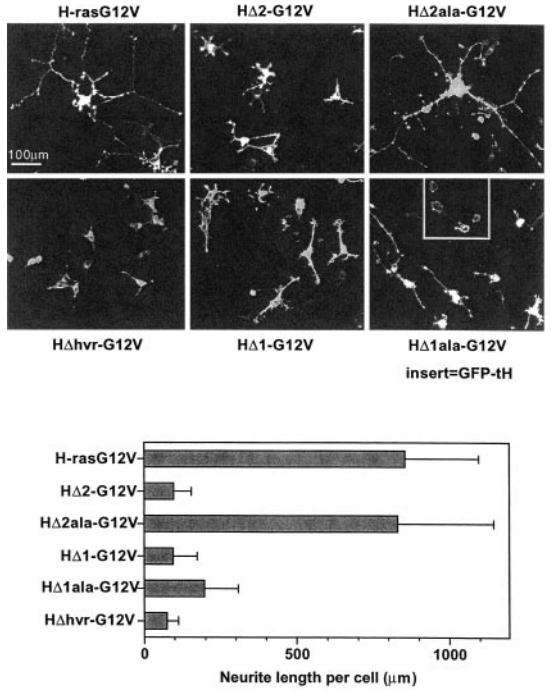


FIG. 4. **Biological activity of Ha-Ras HVR linker mutants.** PC12 cells were transfected with Ha-RasG12V or HVR linker domain mutants tagged with N-terminal GFP. As a negative control, PC12 cells were transfected with GFP-tH. After 48 h, the morphology of the expressing cells was assessed by confocal microscopy. The *upper panel* shows a representative field of PC12 cells expressing each Ras protein. The *lower panel* is a quantification of the extent of neurite outgrowth. The graph shows mean dendrite length per cell (+ S.E.) calculated from measurements on 48–69 cells expressing each Ras protein. Measurements were made using NIH Image software on confocal images of 7 or 8 random fields of cells expressing each Ras protein collected from 3 independent transfections.

pression of HΔ1ala-G12V generated low PI3K activity in the majority of our experiments (as shown in Fig. 3*C*), but in some experiments, higher levels of PI3K activity were detected. The reasons for this variability are unclear. To verify the results of the *in vitro* lipid kinase data, we therefore assessed the activation status of Akt in the same cell lysates by quantitative immunoblotting using phospho-specific antisera. Cells expressing HΔhvrG12V, HΔ1-G12V, HΔ2-G12V, or HΔ1ala-G12V had low levels of phosphorylated Akt both in cell membranes and in cytosol consistent with the profile of PI3K activation (Fig. 3*E*). HΔ2ala-G12V was the only mutant protein capable of activating Akt to the same extent as full-length Ha-RasG12V (Fig. 3*E*).

*Biological Activity of HVR Linker Domain Mutants*—To assess the biological activity of the Ha-RasG12V HVR linker domain mutants, the constructs were tagged with N-terminal GFP and transfected into PC12 cells. After 48 h, the cell cultures were fixed. The morphology of the cells was compared with cells expressing full-length Ha-RasG12V that undergo extensive neurite outgrowth and differentiation and cells expressing membrane-targeted GFP-tH that do not differentiate (GFP-tH consists of the C-terminal 10 amino acids of Ha-Ras cloned onto the C terminus of GFP) (Fig. 4). To quantify the extent of differentiation, mean neurite length was calculated from a random sample of ~50 cells expressing each Ha-Ras protein (Fig. 4). Cells expressing HΔhvrG12V, HΔ1-G12V, or HΔ2-G12V showed some enlargement of the cell body and in some cases the formation of very short neurite-like structures, but the extent of these changes and the complexity of the differentiation was markedly reduced compared with full-length Ha-RasG12V (Fig. 4). The alanine-substituted mutant HΔ1ala-G12V induced slightly more neurite outgrowth than the cognate-deletion mutant. However, only the differentiation induced by HΔ2ala-G12V resembled that observed with full-length Ha-RasG12V. It is clear that the profiles of PC12 differentiation observed in these experiments correlate closely with the biochemical and raft micro-localization data shown in Figs. 2 and 3.

*N-Myristoylation Confines Activated Ha-Ras to Lipid Rafts and Abrogates Raf-1 Activation*—The simplest conclusion to be drawn from the preceding experiments is that preventing the access of activated Ha-Ras to the disordered plasma membrane blocks biological activity. An alternative interpretation is that the linker domain modulates raft association but also directly interacts with plasma membrane-localized Raf-1 and PI3K. We therefore used another mechanism to confine activated Ha-Ras to lipid rafts that did not involve mutating the HVR linker domain. We have previously shown that the addition of an *N*-myristoylation signal to Ha-RasG12V does not interfere with plasma membrane localization. However, sucrose gradient analysis showed that Mys-Ha-RasG12V is extensively localized to lipid rafts (Fig. 5*A*; compare with Fig. 2). Consistent with this observation, assays of raft association based on detergent insolubility showed that membrane-associated Mys-Ha-

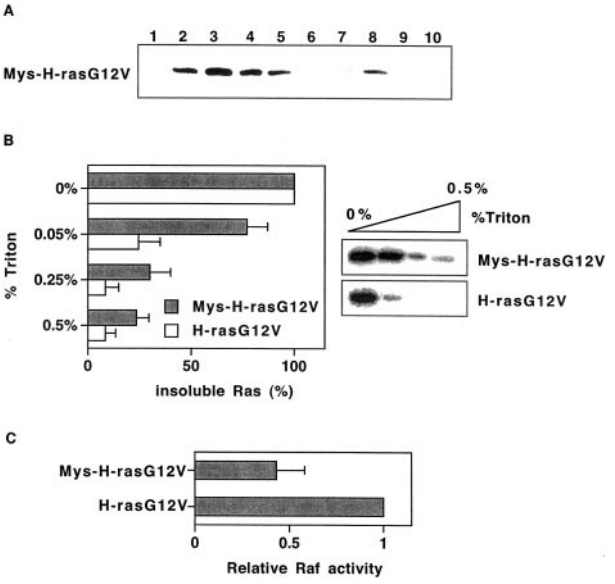


FIG. 5. ***N*-Myristoylation confines activated Ha-Ras to lipid rafts and abrogates Raf-1 activation.** Carbonate lysates of cells transiently expressing Mys-Ha-RasG12V were fractionated over sucrose gradients as in Fig. 2 (*A*). In contrast to non-myristoylated Ha-RasG12V, Mys-Ha-RasG12V localizes exclusively to the lipid raft-containing fractions (compare with Fig. 2). P100 fractions of COS cells transfected with Ha-RasG12V or with Mys-Ha-Ras were solubilized in 0, 0.05, 0.25, or 0.5% Triton X-100 (*B*). P100 fractions were then reisolated by centrifugation and immunoblotted for Ras. The graph shows the mean fraction (%) of Ras (± S.E., $n = 3$) that was detergent-insoluble in each concentration of Triton X-100. P100 fractions from COS cells transfected with Ha-RasG12V or with Mys-Ha-RasG12V were assayed for Raf kinase activity in a coupled MEK-ERK assay (*C*). The graph shows mean relative Raf activity (± S.E.), normalized for Ras expression, that was calculated from 4 independent experiments.

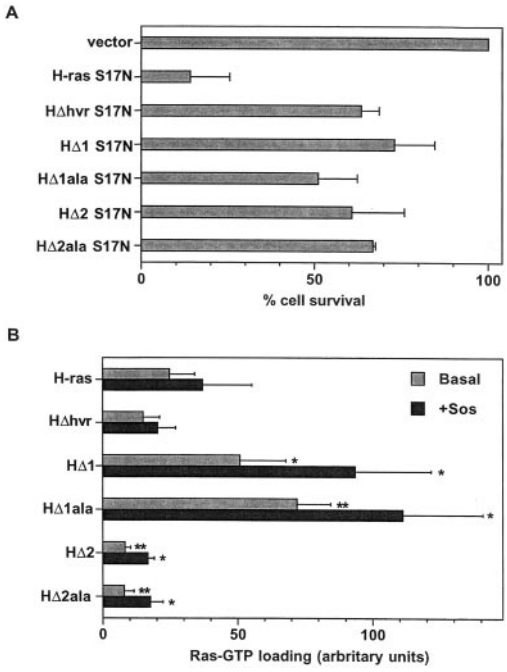


FIG. 6. **Mutation of the Ha-Ras linker domain disrupts interactions with RasGEFs.** An S17N mutation was introduced into the Ha-Ras linker domain mutants (*A*). BHK cells were co-transfected with 10 μg of each S17N expression plasmid together with 0.8 μg of pC1 as selectable marker. Transfections were selected in G418 for 16 days, and the number of colonies was determined after Giemsa staining. The number of surviving cells is expressed as a percentage of the controls that were co-transfected with 10 μg of empty Ras expression vector (EXV) and 0.8 μg of pC1. The results shown are the mean (+ S.E.) of three independent experiments. COS cells were transfected with expression plasmids for wild type Ha-Ras or Ha-Ras linker domain mutants that were wild type (Gly) at codon 12 (*B*). COS cells were also co-transfected with the same Ha-Ras plasmids and 2 μg of mSos1 expression plasmid. Equivalent expression of Sos1 was verified by immunoblotting (not shown). Basal levels and Sos1-stimulated GTP loading of membrane-associated Ha-Ras was then determined using a GST·RBD pull-down assay. The graph shows results (in arbitrary phosphorimaging units) from 3 independent experiments in which each GTP-loading assay was performed in duplicate, and the *bars* show the mean (+ S.E., $n = 6$). The statistical significance of the results was assessed using *t* tests. The wild type basal GTP level was compared with that of each mutant, and the wild type Sos1-stimulated GTP level was compared with that of each mutant. Significant differences are indicated by * ($p < 0.05$) or ** ($p < 0.01$). The degrees of freedom for each *t* test were reduced from 10 to 5 because of the multiple (*i.e.* 5) comparisons made with each control mean.

RasG12V was resistant to extraction in 0.05% Triton X-100, whereas 75% of Ha-RasG12V was solubilized (Fig. 5*B*). Similar to the results obtained with the HVR mutants, raft-associated Mys-Ha-RasG12V was a weaker activator of Raf-1 than Ha-RasG12V (Fig. 5*C*).

*The Interaction of Plasma Membrane-associated Ha-Ras with Exchange Factors Is Altered by Mutations in the HVR Linker Domain*—The S17N mutation results in a Ras protein that forms an irreversible complex with RasGEFs and renders RasS17N dominant negative for cell growth (24). To investigate whether the HVR influences the ability of Ha-Ras to interact with RasGEFs *in vivo*, we introduced the S17N mutation into the Ha-Ras linker domain mutants and assayed them for growth inhibition. BHK cells were co-transfected with S17N-substituted Ha-Ras constructs and pC1, a neomycin resistance plasmid, and selected for 16 days in G418. The number of surviving cells was then compared with control plates transfected with an equivalent amount of empty Ras expression vector. Fig. 6*A* shows that the growth inhibitory phenotype of Ha-RasS17N is markedly reduced in the context of all five linker domain deletions or alanine substitutions. This result strongly suggests that efficient interaction between membrane-associated Ha-Ras and RasGEFs requires an intact HVR linker domain.

To extend this analysis, we assessed directly whether the linker domain influences the sensitivity of Ha-Ras to activation by a specific exchange factor, Sos1. COS cells were transfected with Ha-Ras or the HVR linker domain mutants, all wild type at codon 12, with or without mSos1. The amount of GTP-loaded Ha-Ras protein in the membrane fraction was then determined by a GST·RBD pull-down assay. The basal levels of GTP loading of HΔ2 and HΔ2ala were significantly lower ($p < 0.01$) than wild type Ha-Ras (Fig. 6*B*). Similarly, the levels of GTP loading of HΔ2 and HΔ2ala in cells co-expressing an equivalent low level of mSos1 were all significantly lower ($p < 0.05$) than the GTP loading of full-length Ha-Ras (Fig. 6*B*). These results are what would be expected if the efficiency of interaction of HΔ2 and HΔ2ala with Sos1 is compromised as suggested by the S17N toxicity assays. The basal and Sos1-stimulated GTP loading of HΔhvr were also consistently lower than full-length Ha-Ras, but these differences were not statistically significant ($p < 0.1$). Intriguingly, however, the basal and Sos1-stimulated GTP loading of HΔ1 and HΔ1ala were significantly greater ($p < 0.05$ or $p < 0.01$) than that seen with the corresponding wild type Ha-Ras control (Fig. 6*B*).

## DISCUSSION

Numerous studies published over the last few years have challenged the view that the highly homologous Ha-, Ki-, and N-Ras are functionally redundant. Transgenic experiments have shown that only Ki-Ras is required for normal mouse development (25–27), whereas primary cell culture experi-

ments have shown that N-Ras may have a specific role in suppressing apoptosis (28). In addition, different Ras isoforms transform established fibroblasts with varying efficiencies and exhibit different phenotypes in cell motility and migration assays (29, 30). These biological differences must result from different signal outputs from activated Ha-, N- or Ki-Ras and/or different sensitivities to activation by exchange factors. All three Ras proteins share a common set of GEFs and effectors, yet there are marked quantitative differences in their use of these interacting proteins in intact cells. For example, RasGRF1 activates Ha-Ras more efficiently than N- or Ki-Ras (31), RasGRP2 activates N- and Ki-Ras but not Ha-Ras (23), and mSos1 activates Ras in the hierarchy Ha > N >Ki-Ras.[3] Also, with respect to effector interactions, Ki-Ras is more potent than Ha-Ras at activating Raf-1 and Rac1, whereas Ha-Ras is more potent than Ki-Ras at activating PI3K (29–32). Analysis of Ha/Ki-Ras chimeras has shown that the biological phenotype of the chimeric protein correlates with the origin of the C-terminal HVR (30). Others have shown that perturbing the mechanism of interaction of the C-terminal anchor with the plasma membrane alters the efficiency with which Ha-Ras activates Raf-1 and PI3K (18, 19). These data, taken together with our observations that the Ha-Ras and Ki-Ras C-terminal anchors target to different plasma membrane microdomains, lead to the attractive hypothesis that biochemical and biological differences between the Ras isoforms are due to differences in plasma membrane micro-localization.

The interaction of full-length Ha-Ras with lipid rafts is regulated by GTP loading and is dependent on sequences in the HVR linker domain (16). In the present study, we investigated whether the linker domain modulates Ha-Ras function by directly altering interactions with effectors and GEFs and/or indirectly by altering plasma membrane micro-localization. The deletion analysis shows that, with respect to regulating raft interactions, there are two distinct requirements of the linker domain. Amino acids 173–179 operate as a spacer element because their replacement with alanine residues in HΔ2ala allowed access to the disordered plasma membrane and restored the diminished effector function of HΔ2 back to wild type levels. In contrast, deletion of amino acids 166–172 compromised the normal raft/non-raft equilibrium and effector function of Ha-Ras, and this was not restored by alanine replacement. This suggests that the specific sequence of 166–172 rather than its length is important for regulating Ha-Ras raft association and function.

In Ki-Ras, the sequence corresponding to amino acids 173–179 is taken up by the polybasic domain. This sequence interacts electrostatically with the negatively charged plasma membrane and is in close proximity with the inner leaflet; it is therefore tempting to speculate that the catalytic domains of Ha-Ras may be spaced further away from the inner surface of the plasma membrane than are those of Ki-Ras. Interestingly a recent analysis of the HVR of Ki-RasG12V described two constructs in which a short or long polybasic domain plus a C*AAX* motif was appended directly onto the N-terminal 165 amino acids. Both proteins had a much lower transforming activity than full-length Ki-RasG12V despite both being efficiently localized to the plasma membrane (33). These mutant Ki-Ras constructs effectively have a deletion of the linker domain sequence 166–174; thus specific residues in this region of both Ha- and Ki-Ras appear to be essential for the effector interactions of both Ras proteins. It has not yet been determined, however, whether the microdomain localization of Ki-Ras is altered by deletion of these sequences, as is the case for Ha-Ras.

[3] J. Clyde-Smith and J. F. Hancock, unpublished observations.

Our data show a clear correlation between confinement of Ha-Ras to lipid rafts and defective effector function as measured in Raf-1 and PI3K assays and a cell biological assay of PC12 cell differentiation. Our preferred interpretation is that these observations are related, but it is formally possible that they represent separate phenomena, *i.e.* the linker domain regulates Ha-Ras microdomain association and also has a separate direct role in regulating effector interactions. The results with myristoylated Ha-Ras, however, argue against this alternative hypothesis. N-myristoylated plasma membrane-localized Ha-RasG12V is confined to lipid rafts, in this case because the additional saturated fatty acid facilitates partitioning into liquid-ordered membrane. The linker domain is intact in myristoylated Ha-Ras; therefore the observed defective effector function is most likely due to raft association.

Although Raf activation was compromised by confinement to lipid rafts, downstream activation of MEK and MAPK was apparently unaffected. A similar observation was made recently by Chen and Resh (34), who targeted Raf to lipid rafts using the Src or Fyn N-terminal motifs or to disordered membrane using the Ki-Ras C-terminal targeting motifs. Raf kinase activity *per se* was not assayed in their study, but all three Raf constructs activated MEK and Erk with equal efficiency. A complete explanation of these data is not possible at the present time, although it has been demonstrated by others that the correct coordination of activity within the Raf/MEK/Erk cascade is critically dependent on raft structure and function (35). In addition, it has recently been proposed that internalization of Ras·Raf complexes may be required for efficient activation of MEK and Erk (36). If so, the data in Fig. 3*A* could be rationalized by speculating that raft-associated Raf is more extensively endocytosed than Raf associated with disordered membrane. Notwithstanding the phospho-MEK and phospho-Erk results, the PC12 experiments clearly show that the biological activity of Ha-Ras correlates closely with raft dissociation.

Suppression of the S17N dominant negative phenotype in the context of all five linker domain deletions or alanine substitutions demonstrates that the interaction of RasGEFs with membrane-associated Ha-Ras is critically dependent on the integrity of the linker domain. Unlike the requirements for normal effector function, we cannot safely conclude that any of the Ha-Ras linker domain acts simply as a spacer element for RasGEF binding given that deleted and alanine-substituted proteins were equally compromised. In a co-crystal of the Sos1 catalytic domain with Ha-Ras, the C terminus of Ha-Ras is orientated away from the contact surfaces (37, 38). However, the C-terminal 25 amino acids of Ha-Ras and the non-catalytic domains of Sos-1 were absent from the solved protein complex, so it remains possible that some direct interaction between the Ha-Ras HVR and Sos1 is important for their efficient functional interaction at the plasma membrane. Indeed we have shown previously that prenylated Ras is a better substrate for Sos1 than unmodified Ras *in vitro* (39), observations that also demonstrate that C-terminal Ras epitopes influence N-terminal protein/protein interactions.

Although there was good correlation between the two assays of RasGEF/Ha-Ras interaction with respect to three of the HVR linker domains mutants (Fig. 6, *A* and *B*), this was not the case for HΔ1ala and HΔ1. The increased basal and Sos1-stimulated GTP loading is at variance with the reduced levels expected, as seen with HΔ2ala and HΔ2. One explanation for these results is that the ability of GAP to interact with membrane-associated HΔ1ala and HΔ1 is also compromised. If so, then despite a compromised interaction with Sos1, as demonstrated by the S17N toxicity assay result, HΔ1ala and HΔ1 proteins that are wild type at codon $Gly^{12}$ would still accumulate in the GTP-

bound state. Wild type HΔ1ala and HΔ1, however, do not drive differentiation of PC12 cells (data not shown), presumably because, although GTP-loaded, their effector interactions are also compromised to the same extent as the cognate G12V-substituted proteins. The interaction of p120GAP with the Ha-Ras linker domain mutants is currently being investigated.

In summary, we have shown here that the HVR linker domain modulates the effector, GEF, and possibly GAP interactions of plasma membrane-localized Ha-Ras. There are still some unanswered questions as to how the linker domain mediates these effects, but it is clearly essential for normal Ha-Ras biological function.

*Acknowledgment*—We thank David Bowtell for the mSos1 clone.

REFERENCES

1. Campbell, S. L., Khosravi-Far, R., Rossman, K. L., Clark, G. J., and Der, C. J. (1998) *Oncogene* **17,** 1395–1413
2. Reuther, G. W. and Der, C. J. (2000) *Curr. Opin. Cell Biol.* **12,** 157–165
3. Willumsen, B. M., Christensen, A., Hubbert, N. L., Papageorge, A. G., and Lowy, D. (1984) *Nature* **310,** 583–586
4. Hancock, J. F., Magee, A. I., Childs, J. E., and Marshall, C. J. (1989) *Cell* **57,** 1167–1177
5. Casey, P. J., Solski, P. A., Der, C. J., and Buss, J. E. (1989) *Proc. Natl. Acad. Sci. U. S. A.* **86,** 8323–8327
6. Gutierrez, L., Magee, A. I., Marshall, C. J., and Hancock, J. F. (1989) *EMBO J.* **8,** 1093–1098
7. Hancock, J. F., Paterson, H., and Marshall, C. J. (1990) *Cell* **63,** 133–139
8. Hancock, J. F., Cadwallader, K., Paterson, H., and Marshall, C. J. (1991) *EMBO J.* **10,** 4033–4039
9. Choy, E., Chiu, V. K., Silletti, J., Feoktisitov, M., Morimoto, T., Michaelson, D., Ivanov, I. E., and Philips, M. R. (1999) *Cell* **98,** 69–80
10. Apolloni, A., Prior, I. A., Lindsay, M., Parton, R. G., and Hancock, J. F. (2000) *Mol. Cell. Biol.* **20,** 2475–2487
11. Thissen, J., Gross, J., Subramanian, K., Meyer, T., and Casey, P. (1997) *J. Biol. Chem.* **272,** 30367–30370
12. Chen, Z., Otto, J. C., Bergo, M. O., Young, S. G., and Casey, P. J. (2000) *J. Biol. Chem.* **275,** 41251–41257
13. Roy, M. O., Leventis, R., and Silvius, J. R. (2000) *Biochemistry* **39,** 8298–8307
14. Pol, A., Luetterforst, R., Lindsay, M., Heino, S., Ikonen, E., and Parton, R. G. (2001) *J. Cell Biol.* **152,** 1057–1070
15. Roy, S., Luetterforst, R., Harding, A., Apolloni, A., Etheridge, M., Stang, E., Rolls, B., Hancock, J. F., and Parton, R. G. (1999) *Nature Cell Biol.* **1,** 98–105
16. Prior, I. A., Harding, A., Yan, J., Sluimer, J., Parton, R. G., and Hancock, J. F. (2001) *Nature Cell Biol.* **3,** 368–375
17. Prior, I. A., and Hancock, J. F. (2001) *J. Cell Sci.* **114,** 1603–1608
18. Booden, M. A., Sakaguchi, D. S., and Buss, J. E. (2000) *J. Biol. Chem.* **275,** 23559–23568
19. Coats, S. G., Booden, M. A., and Buss, J. E. (1999) *Biochemistry* **38,** 12926–12934
20. Cadwallader, K., Paterson, H., Macdonald, S. G., and Hancock, J. F. (1994) *Mol. Cell. Biol.* **14,** 4722–4730
21. Roy, S., Lane, A., Yan, J., McPherson, R., and Hancock, J. F. (1997) *J. Biol. Chem.* **272,** 20139–20145
22. Parton, R. G., and Hancock, J. F. (2001) *Methods Enzymol.* **333,** 172–183
23. Clyde-Smith, J., Silins, G., Gartside, M., Grimmond, S., Etheridge, M., Apolloni, A., Hayward, N., and Hancock, J. F. (2000) *J. Biol. Chem.* **275,** 32260–32267
24. Feig, L. A. (1999) *Nature Cell Biol.* **1,** E25–7
25. Johnson, L., Greenbaum, D., Cichowski, K., Mercer, K., Murphy, E., Schmitt, E., Bronson, R. T., Umanoff, H., Edelmann, W., Kucherlapati, R., and Jacks, T. (1997) *Genes Dev.* **11,** 2468–2481
26. Umanoff, H., Edelmann, W., Pellicer, A., and Kucherlapati, R. (1995) *Proc. Natl. Acad. Sci. U. S. A.* **92,** 1709–1713
27. Esteban, L. M., Vicario-Abejon, C., Fernandez-Salguero, P., Fernandez-Medarde, A., Swaminathan, N., Yienger, K., Lopez, E., Malumbres, M., McKay, R., Ward, J. M., Pellicer, A., and Santos, E. (2001) *Mol. Cell. Biol.* **21,** 1444–1452
28. Wolfman, J. C., and Wolfman, A. (2000) *J. Biol. Chem.* **275,** 19315–19323
29. Voice, J., Klemke, R., Le, A., and Jackson, J. (1999) *J. Biol. Chem.* **274,** 17164–17170
30. Walsh, A. B., and Bar-Sagi, D. (2001) *J. Biol. Chem.* **276,** 15609–15615
31. Jones, M. K., and Jackson, J. H. (1998) *J. Biol. Chem.* **273,** 1782–1787
32. Yan, J., Roy, S., Apolloni, A., Lane, A., and Hancock, J. F. (1998) *J. Biol. Chem.* **273,** 24052–24056
33. Welman, A., Burger, M. M., and Hagmann, J. (2000) *Oncogene* **19,** 4582–4591
34. Chen, X., and Resh, M. D. (2001) *J. Biol. Chem.* **276,** 34617–34623
35. Furuchi, T., and Anderson, R. G. (1998) *J. Biol. Chem.* **273,** 21099–21104
36. Rizzo, M. A., Kraft, C. A., Watkins, S. C., Levitan, E. S., and Romero, G. (2001) *J. Biol. Chem.* **276,** 34928–34933
37. Boriack-Sjordan, P. A., Margarit, S. M., Bar-Sagi, D., and Kuriyan, J. (1998) *Nature* **394,** 337–343
38. Chen, J. M., Friedman, F. K., Hyde, M. J., Monaco, R., and Pincus, M. R. (1999) *J. Protein Chem.* **18,** 867–874
39. Porfiri, E., Evans, T., Chardin, P., and Hancock, J. F. (1994) *J. Biol. Chem.* **269,** 22672–22677

# The Linker Domain of the Ha-Ras Hypervariable Region Regulates Interactions with Exchange Factors, Raf-1 and Phosphoinositide 3-Kinase

Montserrat Jaumot, Jun Yan, Jodi Clyde-Smith, Judith Sluimer and John F. Hancock

*J. Biol. Chem. 2002, 277:272-278.*
*doi: 10.1074/jbc.M108423200 originally published online October 31, 2001*

---